CLASSICAL TORQUE ERRORS IN GRAVITY PROBE B EXPERIMENT

A.S.SILBERGLEIT, M.I.HEIFETZ, G.M.KEISER
Gravity Probe B, W.W.Hansen Experimental Physics Laboratory,
Stanford University, Stanford, CA 94305-4085, USA
E-mail: gleit@relgyro.stanford.edu

Classical torques are the first to come into one's mind when thinking about sources of systematic errors in Gravity Probe B (GP-B) Relativity Science Mission, which is why they have been most thoroughly investigated. In this paper we give a brief survey of these studies and their results. First, the classification of all known non-relativistic torques that is used in the GP-B Error Tree is given, and the Error Tree spreadsheet is described. Second, the theory of electrostatic support dependent torques is outlined, including the universal expression for the housing-fixed components of the torques, the definition of the fifteen torque coefficients and their relation to the rotor shape. Examples of the final formulas for the drift rates of several particular support dependent and support independent torques are presented. Finally, contributions of different groups of torques to the total expected experimental error are compared, and the top contributing torques are discussed.

1 Introduction

The Gravity Probe B satellite, which is planned to fly in the year 2000, contains a set of high-precision superconducting gyroscopes (the outline of the GP-B experiment is given in [1]). They are to test the predictions of general relativity that a gyroscope in a low (altitude$\approx$ 650 km) circular polar orbit will precess about 6.6 *arcsec/year* in the orbital plane (geodetic precession, East-West (EW) direction) and about 42 *milliarcsec/year* perpendicular to the orbital plane (frame-dragging precession, North-South (NS) direction; for the theory of both effects, see c. f. [2]). The required total error of the gyro drift rate determination is 0.5 *milliarcsec/year*; we expect even a better accuracy, about few parts in 10^5 for the measurement of the geodetic effect.

Non-relativistic torques on the GP-B gyroscopes had been primarily considered as the most important source of experimental errors; that is why the experimental hardware is required to provide the performance allowing not more than 0.3 *milliarcsec/year* contribution of all the classical torques. To prove that this is possible, as well as to develop proper verification procedures, the classical torques have therefore been extensively investigated for a long time. Earlier GP-B classical torque studies are reported in [3]; this paper is a brief survey of state of the art results from [4] and [5]. A large part of it is devoted

to the theory of electrostatic torques as developed in [4]; unlike the previous versions, it is based mostly on symmetry considerations and thus avoids lengthy technical complications characteristic of earlier approaches (see sec. 3).

2 GP-B Error Tree and Classification of Non-Relativistic Torques

There are two different types of torques: support dependent (SD) torques, which are caused by control voltages of the electrostatic gyro suspension system, and support independent ones (SI), which act on the gyro even if it is not supported (the torques due to position bridge voltages belong here). Extensive results on torques of either group are given in [4] and [5], respectively.

A complete classification of all non-relativistic torques and evaluation of the gyro drift caused by them is done in the GP-B New Error Tree (NET) (see [6], [7]) implemented as an Excel spreadsheet workbook. The NET consists of two main parts describing non-relativistic drifts and measurement (read-out) errors, respectively. The NET is a 'live' one, i. e., one only has to specify (type in) numerical values of all necessary parameters in the 'input' sheets (*"Constants"*, *"Parameters"*, *"Coefficients"*, *"Preloads"*, and, partly, *"Accelerations"* and *"Accelerations Squared"*), and the values of all classical drift rates are immediately computed by the spreadsheet. After combining the result with the measurement error and the uncertainty in the proper motion of the Guide Star, the total experimental error is also calculated. The three resulting errors and their total (in *milliarcsec/year*) are seen in the 'top' sheet of the NET, fig. 1, for the drift rate in the NS and EW directions (the way those totals are computed is explained below).

Each error there and in all boxes of all the 'lower level' sheets is represented by two numbers corresponding to the so called worst and plausible case, respectively. The numbers are calculated from a different sets of parameters in the input sheets mentioned above (only the table *"Constants"* contains one set of values, because those are either fundamental constants, like the speed of light, or have a well specified value in the GP–B project, such as the rotor radius). The total number of parameters is around one hundred. The worst case values are either taken directly from the requirements, or derived from them, or else are the result of our estimate of what the worst case value may be for a particular parameter in reality. The plausible case values either are already achieved experimentally, or are expected to be achieved 'with the 99%' certainty. So, the plausible case shows what we strongly expect to have in the real experiment, while the worst case represents the upper bound of errors: they definitely are not going to be worse than that if all the hardware works as required. Naturally, the NET book is arranged in such way that a change

of a worst case value automatically implies variations of dependent worst case values *only*, not affecting the plausible case at all, and vice versa.

The principal classification of the torques is found in the next (after the 'top' one) sheet of the NET shown in fig. 2, along with the drift rate contribution of each particular group of torques. SD torques are first subdivided in two major groups. The first group contains the torques which depend on accelerations, i. e., which stem from how the suspension system reacts to the forces applied to the gyro when trying to keep it centered. The second group consists of torques which depend on the preloads, in other words, on the voltages provided by the suspension system when it is just turned on, even if no force at all is acting on the gyro. The next subdivision in both major groups is related to the rotor's *position* in which the torques are produced, namely, the *nominal*, *misaligned*, and *miscentered* position. (We call the rotor's position nominal when the rotor is perfectly centered in the housing and its spin axis is aligned with the roll axis of the spacecraft; accordingly, in the misaligned position there is an angle between the spin and roll axes, while in the miscentered position the center of mass of the rotor is displaced from the center of the housing.)

Therefore there are exactly $6 = 2 \times 3$ sheets with SD torques from *"Sheet 1"* (acceleration dependent, nominal position torques) to *"Sheet 6"* (preload dependent, miscentered position torques). In each of the sheets, torques are again subdivided into several larger groups, such as those caused by accelerations either parallel or perpendicular to the spacecraft roll axis, or by preloads or preload differences, etc. Finally, the torques are sorted out by their physical source, and every such particular torque is represented by its own 'lowest level' box. There are over a hundred of different torques in the NET now; even more are known, but quite a few of them are not included in the NET because their contribution turns out to be entirely negligible.

The boxes are connected by lines in an ascending way, so that the structure of every sheet with torques is that of a tree graph: each box of a lower level is connected to a single upper level box. An example of *"Sheet 2"* with acceleration dependent, misaligned position SD torques is shown in fig. 3; this sheet has been chosen because its structure is rather simple, other sheets include more branches and boxes than that one.

SI torques are first classified as housing fixed and inertially fixed, fig. 2. The former (sheets 7–9) are again sorted relative to the nominal, misaligned and miscentered rotor's position; all inertially fixed torques are listed in sheet 10. Particular SI torques are dealt with in each of the sheets 7–10 in a similar manner as SD torques in sheets 1–6, except that the grouping is done now by the physical origin of the torques (electrostatic, magnetis, etc.). As an

example, *"Sheet 7"* with SI, housing-fixed, nominal position torques is shown in fig. 4.

All the ten sheets with the torques are filled in in the following way. The lowest level boxes of every sheet show drift rates due to a torque which belongs to some particular group and is caused by a particular physical source. The four values of drift rates given in the box (NS worst, NS plausible, EW worst, EW plausible) are calculated by the proper formula from [4] or [5] in which either worst or plausible values of the pertinent parameters from the input sheets are used. As soon as the values of all the input quantities are specified, the numbers appear in the lowest level boxes, as well as in all upper level ones, all the way up to the top sheet shown in fig. 1. The numbers in the upper level boxes are automatically computed by means of a built-in procedure operating by the rule based on the assumption that different torques act independently. So, say, the squares of EW, worst case drift rates from all the boxes of a group at any given level are summed up, and the square root of this sum is inserted as a value of EW, worst case drift rate into the next level box to which the group is attached. This operation is repeated level after level from the bottom to the top of a given sheet with torques, which results in the numbers given in the uppermost box of the sheet representing the combined contribution of all the torques included in it (for instance, SD, acceleration dependent, misaligned position torques from *"Sheet 2"* in fig. 3). Those uppermost boxes of sheets 1–10 serve as the lowest level boxes of the sheet in fig. 2, whose uppermost box, containing the total drift rate from all classical torques, serves, in its turn, as one of the three lowest level boxes of the top sheet (fig. 1), along with the box containing the total measurement error and the other one with the contribution of proper motion of the Guide Star.

So, one needs some formulas to calculate every separate 'lowest level' torque; in the next two section we outline their derivation as given in [4], [5] and discuss various related questions.

3 Theory of Support Dependent Torques

3.1 Derivation of Housing-Fixed SD Torques

GP-B gyro suspension system consists of three pairs of electrodes (labeled $a_\pm$, $b_\pm$, $c_\pm$) positioned symmetrically as shown in fig. 5. Cartesian coordinates $\{x, y, z\}$ are fixed in the housing, with the $\hat{\mathbf{z}}$ unit vector pointed in the direction of the roll axis of the spacecraft. Thus the unit vectors to the centers of the electrodes are given by

$$\hat{\mathbf{e}}_{a\pm} = \mp\frac{\sqrt{2}}{2}(\hat{\mathbf{y}} - \hat{\mathbf{z}}); \qquad \hat{\mathbf{e}}_{b\pm} = \pm\frac{\sqrt{2}}{2}(\hat{\mathbf{y}} + \hat{\mathbf{z}}); \qquad \hat{\mathbf{e}}_{c\pm} = \pm\hat{\mathbf{x}} \qquad (1)$$

The first complete and consistent derivation of GP-B SD torques had been carried out by G.M. Keiser in [9], whose approach was independently checked later in [10]. An approximate explicit expression for the capacitance and a rather complicated technique of spherical harmonics and rotation matrices was used there. Here we follow another version of the theory developed in [4] which is based on the symmetry arguments and thus avoids explicit expression of the capacitance (until the very end, when the torque coefficients are calculated, see sec. 2.4), allowing one to establish the structure of SD torques without it.

The calculation of SD torques starts with the general formula for an electrostatic torque acting on a conducting body (c. f. [8], 3.14, (6)):

$$\mathbf{T} = \frac{1}{2} V^2 \frac{\partial C}{\partial \eta} \hat{\eta}, \tag{2}$$

which is a direct implication of the energy conservation. Here V is the electrode to rotor potential, C is the electrode to rotor capacitance, and η is the rotation angle about the direction $\hat{\eta}$.

The orientation of the rotor may be described by any three Euler angles α, β, γ. It is convenient to choose them as shown in fig. 6 , so that α and β specify the position of the gyro spin axis, $\vec{\omega}_s = \omega_s \hat{\mathbf{s}}$, relative to the housing, while γ represents rotation about $\vec{\omega}_s$. Since $\hat{\mathbf{z}}$ points along the roll axis, the angle β is the spin–roll axes misalignment. The spin axis unit vector is given, evidently, by

$$\hat{\mathbf{s}} = \hat{\mathbf{s}}(\alpha, \beta) = (\hat{\mathbf{x}} \cos\alpha + \hat{\mathbf{y}} \sin\alpha) \sin\beta + \hat{\mathbf{z}} \cos\beta$$

By applying formula (2) to each of the Euler angles for any electrode and then projecting the obtained equalities on the $\{x, y, z\}$ axes using

$$\hat{\alpha} = \hat{\mathbf{z}}, \quad \hat{\beta} = -\hat{\mathbf{x}} \sin\alpha + \hat{\mathbf{y}} \cos\alpha, \quad \hat{\gamma} = (\hat{\mathbf{x}} \cos\alpha + \hat{\mathbf{y}} \sin\alpha) \sin\beta + \hat{\mathbf{z}} \cos\beta,$$

for the housing-fixed components of the torque we obtain:

$$T_x = \frac{1}{2} V^2 \left(-\sin\alpha \frac{\partial C}{\partial \beta} - \cos\alpha \cot\beta \frac{\partial C}{\partial \alpha} + \frac{\cos\alpha}{\sin\beta} \frac{\partial C}{\partial \gamma} \right)$$

$$T_y = \frac{1}{2} V^2 \left(\cos\alpha \frac{\partial C}{\partial \beta} - \sin\alpha \cot\beta \frac{\partial C}{\partial \alpha} + \frac{\sin\alpha}{\sin\beta} \frac{\partial C}{\partial \gamma} \right) \tag{3}$$

(we are not interested here in the torque T_z which changes the rotor spin speed, so we do not give its expression). The primary simplification of these formulas comes from the first of our three basic assumptions. All the assumptions are

good approximations under the GP-B conditions, and they were used in all the previous versions of the theory, sometimes implicitly.

Assumption 1 (spin averaging) *Instantaneous spin axis direction* $\hat{\mathbf{s}}$ *coincides with the (inertially fixed) direction of the angular momentum; the voltage does not vary at the spin frequency.*

Under Assumption 1, the torques (3) averaged over the rotation of the rotor become

$$T_x^i = -\frac{1}{2}V_i^2\left(\sin\alpha\,\frac{\partial C^i}{\partial\beta} + \cos\alpha\cot\beta\,\frac{\partial C^i}{\partial\alpha}\right)$$

$$T_y^i = \frac{1}{2}V_i^2\left(\cos\alpha\,\frac{\partial C^i}{\partial\beta} - \sin\alpha\cot\beta\,\frac{\partial C^i}{\partial\alpha}\right); \qquad (4)$$

the index i enumerates the electrodes, $i = a_\pm,\ b_\pm,\ c_\pm$; C^i is the spin averaged value of the capacitance which, given a real rotor shape, depends on the rotor's position in the housing. The latter can be described by the misalignments relative to the housing-fixed axes,

$$\theta_x = \sin\beta\cos\alpha \simeq \beta\cos\alpha \qquad \theta_y = \sin\beta\sin\alpha \simeq \beta\sin\alpha$$

which are small because $\beta \sim 10^{-5}$ in GP-B, and another small parameter, the relative miscentering, $\mathbf{r}_\circ = (x_\circ\,\hat{\mathbf{x}} + y_\circ\,\hat{\mathbf{y}} + z_\circ\,\hat{\mathbf{z}})/d$. Here d is the nominal gap between the rotor and the housing, and vector $\mathbf{r}_\circ$ goes from the geometrical center of the housing to the rotor's center of mass.

So, generally, $C^i = C^i(\alpha, \beta, \mathbf{r}_\circ)$, and we need its derivatives in the angles involved in (4) to the first order in β (or θ_x, θ_y) and $r_\circ = |\mathbf{r}_\circ|$. According to our classification of torques, the derivatives are needed for the three positions of the rotor: *1) nominal position,* ($\beta = 0, \quad r_\circ = 0$); *2) misaligned position,* ($\beta \neq 0$, small; $r_\circ = 0$); *3) miscentered position,* ($\beta = 0; \quad r_\circ \neq 0$, small). Of course, no progress can be made unless we somehow restrict the functional dependence $C^i(\alpha, \beta, \mathbf{r}_\circ)$. The suitable restriction can be formulated as

Assumption 2 *The spin-averaged electrode-to-rotor capacitance depends only on the angle between the spin and electrode axes, and on two projections of miscentering on those directions:*

$$C^i = C^i(\xi_i,\ \lambda,\ \mu_i), \qquad i = a_\pm,\ b_\pm,\ c_\pm$$

where $\xi_i = \hat{e}_i \cdot \hat{\mathbf{s}}, \quad \lambda = \hat{\mathbf{s}} \cdot \mathbf{r}_\circ, \quad \mu_i = \hat{e}_i \cdot \mathbf{r}_\circ.$

This is a natural conjecture confirmed by direct calculations in [9], [10]; it reduces the number of independent arguments of function C^i from five to three.

Assumption 2 allows us to essentially simplify $\partial C^i/\partial\alpha$, $\partial C^i/\partial\beta$ and to write the housing–fixed torques for the three positions as follows:

$$\mathbf{T}^i_{nom} = \frac{V_i^2}{2}\tilde{K}^i\left[-(\hat{e}_i\cdot\hat{\mathbf{y}})\hat{\mathbf{x}} + (\hat{e}_i\cdot\hat{\mathbf{x}})\hat{\mathbf{y}}\right] \tag{5}$$

$$\mathbf{T}^i_{misal} = \frac{V_i^2}{2}\Big\{\tilde{K}^i(\hat{e}_i\cdot\hat{\mathbf{z}})(\theta_y\hat{\mathbf{x}} - \theta_x\hat{\mathbf{y}}) + \tilde{L}^i\left[-(\hat{e}_i\cdot\hat{\mathbf{y}})^2\theta_y\hat{\mathbf{x}} + (\hat{e}_i\cdot\hat{\mathbf{x}})^2\theta_x\hat{\mathbf{y}}\right]\Big\} \tag{6}$$

$$\mathbf{T}^i_{misc} = \frac{V_i^2}{2}\Big\{\tilde{D}^i_1\left(-\frac{y_o}{d}\hat{\mathbf{x}} + \frac{x_o}{d}\hat{\mathbf{y}}\right) + \left[\tilde{D}^i_2\frac{z_o}{d} + \tilde{D}^i_3(\hat{e}_i\cdot\mathbf{r}_o)\right]\left[-(\hat{e}_i\cdot\hat{\mathbf{y}})\hat{\mathbf{x}} + (\hat{e}_i\cdot\hat{\mathbf{x}})\hat{\mathbf{y}}\right]\Big\} \tag{7}$$

$$\tilde{K}^i = \frac{\partial C^i}{\partial\xi_i},\quad \tilde{L}^i = \frac{\partial^2 C^i}{\partial\xi_i^2},\quad \tilde{D}^i_1 = \frac{\partial C^i}{\partial\lambda},\quad \tilde{D}^i_2 = \frac{\partial^2 C^i}{\partial\lambda\partial\xi_i},\quad \tilde{D}^i_3 = \frac{\partial^2 C^i}{\partial\mu_i\partial\xi_i}; \tag{8}$$

the derivatives here are taken at $\beta = 0$, $\mathbf{r}_o = 0$.

This is an intermediate answer, and it looks rather simple. However, there are still 30 coefficients involved in it; our last assumption, which has always been used in GP-B, slashes their number twice.

Assumption 3 (electrode symmetry) *Capacitances between electrodes and rotor averaged over the spin period, as functions of their arguments, coincide pairwise:*

$$C^{c+}(\xi,\lambda,\mu) \equiv C^{c-}(\xi,\lambda,\mu) \equiv C(\xi,\lambda,\mu)$$
$$C^{a+}(\xi,\lambda,\mu) \equiv C^{b+}(\xi,\lambda,\mu) \equiv C^{+}(\xi,\lambda,\mu)$$
$$C^{a-}(\xi,\lambda,\mu) \equiv C^{b-}(\xi,\lambda,\mu) \equiv C^{-}(\xi,\lambda,\mu)$$

According to this assumption and the definitions (8), the number of coefficients is reduced by way of

$$K^{c+} = K^{c-} \equiv K,\quad K^{a+} = K^{b+} \equiv K^{+},\quad K^{a-} = K^{b-} \equiv K^{-}$$
$$L^{c+} = L^{c-} \equiv L,\quad L^{a+} = L^{b+} \equiv L^{+},\quad L^{a-} = L^{b-} \equiv L^{-},$$

etc.

Using the new and consistently denoted coefficients, the housing-fixed torques (5)–(7) in all the three positions can be written as sums of terms of the standard form:

$$K_\nu \times \left(V_{i+}^2 \pm V_{i-}^2\right) \times \Big(\text{position factor}\Big), \qquad i = a, b, c, \tag{9}$$

where the position factor equals to 1 for the nominal position, to one of the misalignments θ_x, θ_y for the misaligned position, and to some projection of the miscentering $\mathbf{r}_o$ for the miscentered position; K_ν, $\nu = 1, 2, \ldots, 15$ are the fifteen torque coefficients studied in sec. 2.4.

3.2 *SD Torques in the Inertial Frame. Relation to Accelerations and Preloads*

To obtain the final formulas for the drift rates used in the NET from the expressions for the housing-fixed torques based on (9), one needs to 1) transform the torques to the inertial frame; 2) relate the squares of voltages to either accelerations or preloads (and specify the latter); 3) average the result over the roll period.

The first step, though cumbersome, is otherwise straightforward, since, with enough accuracy, we can consider the inertial frame just rotating with the roll frequency about the z axis of the housing-fixed frame. At the second step we make use of the expression for the net force on the gyro exerted by a pair of electrodes [8] which relates thus the differences of squares of opposite electrode voltages to the acceleration g (see [9]):

$$V_{i+}^2 - V_{i-}^2 = -A\,g, \quad A = m_g \frac{8d^2}{\pi\epsilon_0 r_g^2} \simeq 5.09 \times 10^4\ volts^2/m\,sec^{-2}$$

(m_g and r_g are the mass and radius of the rotor). The corresponding sums, on the other hand, define the preload acceleration h_i according to

$$V_{i+}^2 + V_{i-}^2 = \frac{1}{2} A \left(h_i + \frac{g^2}{h_i} \right)$$

(acceleration is also involved here, but typically the second term on the r. h. s. is much smaller than the first one. Nevertheless, such terms are also taken care of in the NET, and the inclusion of the input sheet *"Accelerations squared"* is caused by them). The values of preloads are specified by GP-B requirements; the exhaustive list of forces acting on the GP-B gyro (and the expressions for the corresponding accelerations used in the NET) has been compiled in [11]; its shorter version is also found in [4].

The roll averaging is significantly complicated by the fact that, along with the D.C. components, accelerations, preloads *and* the miscentering may also vary at roll, twice roll, and some other frequencies, which variations generally do contribute to the average SD torques. That is why even the list of expressions for the averaged inertial SD torques in terms of voltages (and not yet accelerations and preloads!) occupies almost five pages in [4]; it is thus not included here. Instead, we give just two examples of the final expressions for the drift rates which are typical in their structure and, we think, give one a good idea of all the formulas exploited in the lowest level boxes of sheets 1–6 of the NET.

3.3 *Two Examples of Formulas for SD Torques*

For brevity, we give the expressions only for the East–West (geodetic) component, $\dot{EW}$, of the drift rate; the North–South component looks absolutely similar.

1. Preload dependent, nominal position torque due to variation of preload difference $h_a - h_b$ at roll (NET sheet 4, box 1.2.1; see fig. 4) Here

$$\dot{EW} = \frac{K_3}{I\omega_s}\langle (V^2)_a^+ - (V^2)_b^+ \rangle_{co} = \frac{K_3}{I\omega_s}\frac{A}{4}(h_{ac} - h_{bc}),$$

where I is the moment of inertia, h_{ic} is the amplitude at cosine of roll of the i-th preload, we denote $(V^2)_i^{\pm} \equiv V_{i+}^2 \pm V_{i-}^2$, and the angle brackets mean the averaging over the roll period with the factor of either cosine (*'co'*) or sine (*'si'*) of the roll phase.

2. Acceleration dependent, nominal position torque due to Earth gravity gradient (NET sheet 1, box 1.2.1) In this case

$$\dot{EW} = -\frac{K_1}{I\omega_s}\langle (V^2)_c^- \rangle_{co} + \frac{K_4}{I\omega_s}\langle (V^2)_a^- - (V^2)_b^- \rangle_{si} = \frac{K_1 + K_4\sqrt{2}}{I\omega_s}\frac{A}{2}g_e$$

where the acceleration g_e is given by ([11], [4])

$$g_e = \frac{3\mu_e D}{16R^3} J_2 \left(\frac{R_e}{R}\right)^2 \sin 2\delta$$

Here μ_e is GM value for Earth, D is the distance of the gyro in question to the unsupported gyro, J_2 is the Earth oblateness, R_e is the Earth radius, R is the orbital radius, and δ is the declination of the Guide Star.

Same as these two, all the final expressions of the drift rates are sums of ratios of products of various input parameters.

3.4 *Torque Coefficients and the Rotor Shape*

To finish with the SD torques, it remains only to describe how the torque coefficients are evaluated. Suppose that the exact shape of the rotor is known in terms of the spherical harmonics expansion,

$$r = R(\theta', \varphi') = \sum_{l=0}^{\infty} \sum_{m=-l}^{l} r'_{lm} Y'_{lm} \equiv \sum_{l,m} r'_{lm} Y'_{lm} \qquad (10)$$

Here the primed frame is fixed in the body of the rotor, r'_{lm} are called the rotor shape coefficients, and

$$Y'_{lm} = Y_{lm}(\theta', \varphi'); \quad Y_{lm}(\theta, \varphi) = \sqrt{\frac{2l+1}{4\pi}\frac{(l-m)!}{(l+m)!}}\, P_l^m(\cos\theta) e^{im\varphi};$$

$P_l^m(\cos\theta)$ are the Legendre functions. If the spin axis is oriented along the z' axis, which is, we emphasize, randomly fixed in the body when measuring the shape, i. e., if $\hat{\mathbf{s}} = \hat{\mathbf{z}}'$, then, as shown in [4],

$$K'_i = \kappa \sum_{l=even/odd,\, l>0} \hat{K}_i(l) r'_{l0} \quad i = 1, 2, \ldots, 15; \qquad \kappa = \frac{\varepsilon_0 r_g^2}{2d}, \qquad (11)$$

where $\hat{K}_i(l)$ are known functions of l, such as

$$\hat{K}_1(l) = \sqrt{\frac{\pi}{2l+1}}\, P_l^1(0) \left[P_{l-1}\left(\sqrt{3}/2\right) - P_{l+1}\left(\sqrt{3}/2\right)\right], \qquad l > 0,$$

etc. (the complete list of expressions for the multipliers $\hat{K}_i(l)$ is found in [4]). Note that no electrostatic torque acts on a perfect sphere, and, accordingly, no $l = 0$ term with $r'_{00} = \sqrt{4\pi} r_g$ is present in (11).

However, we need to know the torque coefficients for an *arbitrary* orientation of the spin axis in the body of the rotor, that is, when the unit spin vector $\hat{\mathbf{s}}$ is at any Euler angles α, β to the body fixed axis z'. The problem of their determination was solved in [12] with the result (* means complex conjugate):

$$K_i(\alpha, \beta) = \kappa \sum_{l=even/odd,\, l>0} \hat{K}_i(l) \left(\frac{4\pi}{2l+1}\right)^{1/2} \sum_{m=-l}^{l} r'^{*}_{lm} Y_{lm}(\alpha, \beta) \qquad (12)$$

Analytical formulas for the torque coefficients including polhode motion of the spin axis are also obtained in [12]; they prove that polhoding reduces torque coefficients and thus the total drift error.

The only difficulty with using the formula (12) in practice is that it is impossible to precisely measure the shape of the coated GP-B flight rotors without a serious damage to the rotor's surface. To circumvent that, three coated GP-B flight class gyros have been anodized, to strengthen their surface layer, and then their shape was measured, giving the set of the rotor shape coefficients r'_{lm}, $l \leq 16$ for each ball. Then the torque coefficients as functions of the spin axis position in the rotor's body have been tabulated by means of formula (12). Thus, the ranges of their variation with the spin axis direction

have been determined. The details of this study, as well as the theoretical analysis of the torque coefficients, are given in [12]. Here we emphasize the following results: 1)the mass unbalance ($l = 1$) due to nonuniformity of the rotor coating extends the ranges of odd harmonics torque coefficients; 2)the centrifugal asphericity ($l = 2$) due to the equatorial bulge of the spinning rotor just shifts the ranges of even harmonics torque coefficients; 3) with the measured mass unbalance and centrifugal asphericity included, all the three rotors meet the GP-B requirements on the classical drift with a good margin (almost an order of magnitude for the plausible case). The last result is obtained, naturally, with the help of the NET.

4 Remarks on Support Independent Torques

In contrast with SD torques, it is impossible to develop a uniform theory of SI torques on the GP-B gyro, because of the difference in their physical origin. With this lack of a unifying structure behind, we face a large variety of SI torque derivations collected in [5]. One can though detect some similarities in calculation of torques of the same physical nature, such as electrostatic, magnetic, differential damping torques, etc. Our first point here is that several electrostatic SI torques are expressed in terms of the same torque coefficients as the SD torques. For example, let us consider

1. *Housing fixed, misaligned position electrostatic torque due to rotor charging.* The drift rates caused by it are shown to be

$$\dot{EW} = -2NS_0 \frac{K_2 + 2K_5}{I\omega_s} V_r^2, \qquad \dot{NS} = 2EW_0 \frac{K_2 + 2K_5}{I\omega_s} V_r^2,$$

where V_r is the rotor to ground potential, and NS_0, EW_0 are the NS and EW misalignments, respectively.

As another example of the SI torques we present the largest of them, namely

2. *Housing fixed, misaligned position magnetic torque due to coupling of the London moment (M_L) with the local shield.* In this case the drift rates have been originally calculated in [13] as

$$\{\dot{EW}, \dot{NS}\}^T = 7.6 \times 10^6 \frac{\mu_0 M_L^2}{I\omega_s R_0^3} \{NS_0, EW_0\}^T,$$

where R_0 is the pick-up loop radius, the misalignments are in *marcsec*, and the numerical coefficient produces the answer in *marcsec/yr* as soon as all other quantities in the r.h.s. are in the MKS units.

An interesting example of calculation of the torque caused by eddy currents in normal metals surrounding the rotor due to the magnetic field of fluxons on the rotor's surface may be found in [14].

5 Discussion. Top Contributing Torques

The 'top' sheet of the NET in fig. 1 shows that our estimates of the drift caused by the classical torques in both the worst and plausible case meets the GP-B requirement of $0.3\,marcsec/yr$ with a good margin. It also demonstrates that the largest expected GP-B error is the measurement error (see [15] for details), and that the classical torques contribution is on the level of the uncertainty in the Guide Star proper motion.

From the sheet with the non-relativistic drift in fig. 2 it is clear that the contribution of the SD torques dominates that of the SI torques, and that the nominal position, preload dependent torques lead among the former.

Finally, the top torques contributing to the drift in either direction are found in the table in fig. 7, also taken form the NET. The selection includes all torques with the drift rate larger than 0.001 *marcsec/yr*. It is seen that only two of eight (EW) or nine (NS) top torques are support independent ones, and only one of them (given in the previous section) makes the third place in the case of the NS drift.

The torques listed in fig. 7 provide well over 99% of the classical drift rate, and only seven of the fifteen torque coefficients are involved in them. Moreover, the contribution of only three largest torques is slightly below 99%, and just three torque coefficients and few other parameters are present in their expressions. On the one hand, this fact makes our estimates of the torques 'robust', that is, less sensitive to parameter changes; on the other hand, it indicates priorities of the post-flight verification regarding non-relativistic torque errors of the experiment.

Acknowledgments

This work was supported by NASA grant NAS 8-39225 to Gravity Probe B. We would like to appreciate the efforts of many people who have contributed, over two decades, to the study of classical torques on the GP-B gyros: Penny Axelrad, Brian DiDonna, Francis Everitt, Dale Gill, Christian Gothier, Jeremy Kasdin, Jim Lockhart, Frane Marcelja, John Turneaure, Richard Vassar, Todd Walter.

References

1. G.M.Keiser in *These Proceedings.*
2. R.J.Adler, A.S.Silbergleit in *These Proceedings.*
3. C.W.F.Everitt, *Report on a Program to Develop a Gyro Test of General Relativity in a Satellite and Associated Control Technology*, Stanford University, Stanford, 1980.
4. G.M.Keiser, A.S.Silbergleit, *New Error Tree: Support Dependent Torques*, (GP-B doc. S0263, Stanford University, 1998).
5. G.M.Keiser, A.S.Silbergleit, *New Error Tree: Support Independent Torques*, (GP-B doc. S0264, Stanford University, 1996).
6. G.M.Keiser, M.I.Heifetz, A.S.Silbergleit, *New Live Error Tree*, (GP-B doc. S0292, Stanford University, 1998).
7. M.I.Heifetz, C.W.F.Everitt, G.M.Keiser, A.S.Silbergleit, in *Proc. of the 8th Marcel Grossman Meeting on General Relativity*, (in press).
8. W.R.Smythe, *Static and Dynamic Electricity*, 3rd edition, (Hemisphere Publ. Corp., New York, Washington, Philadelphia and London, 1989).
9. G.M.Keiser, *Suspension Torques on a Gimballed Electrostatically Supported Gyroscope and Requirements on the Gyroscope and Spacecraft for the Relativity Gyroscope Experiment*, (GP-B doc. S0019, Stanford University, 1985).
10. B.DiDonna, *Suspension Torque Prediction for the Relativity Gyroscope Experiment*, (Undergraduate Honors Thesis, Dept. of Physics, Stanford University, 1994).
11. G.M.Keiser, *Non-Relativistic Forces Acting on GP-B Gyroscopes*, (GP-B doc. S0269, Stanford University, 1996).
12. A.S.Silbergleit, *GP-B Rotor Shape and Torque Coefficients*, (GP-B doc. S0289, Stanford University, 1998).
13. L.B.Holdeman, J.T.Holdeman, Jr., J. Appl. Phys. **57**, 584 (1980).
14. G.M.Keiser, A.S.Silbergleit, Techn. Phys. **43**, 131 (1998).
15. M.I.Heifetz, G.M.Keiser, A.S.Silbergleit in *These Proceedings.*

Gravity Probe B Error Tree

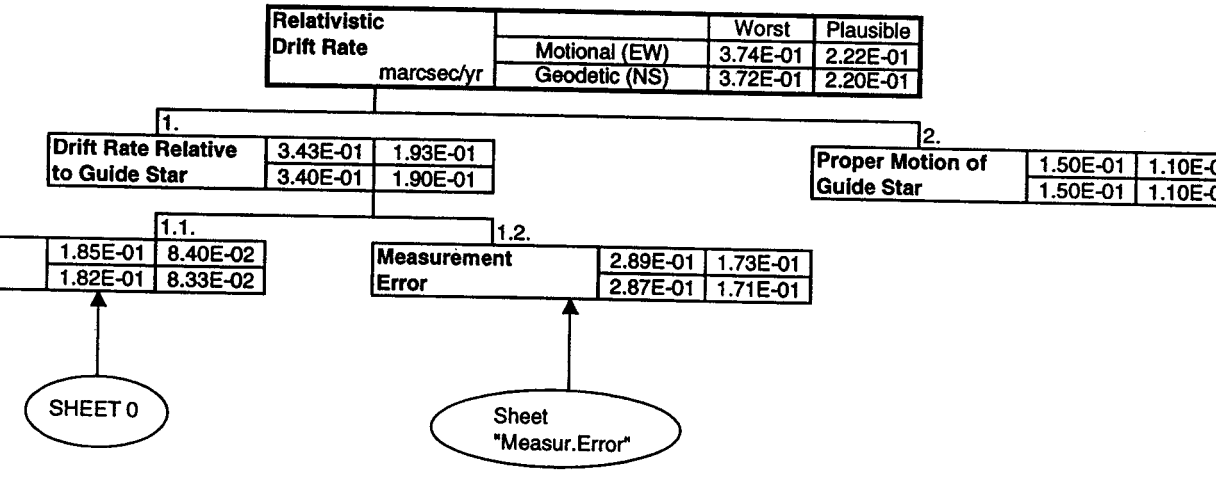

Fig. 1. `Top' sheet of the NET

Non - Relativistic Drift

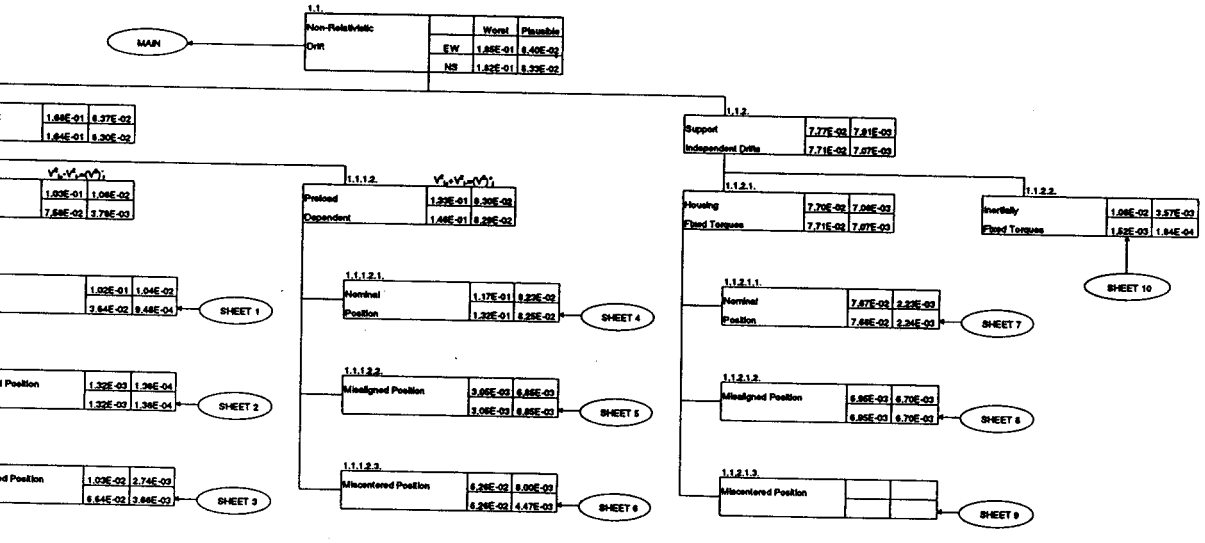

Fig. 2

Acceleration Dependent, Misaligned Position Torques

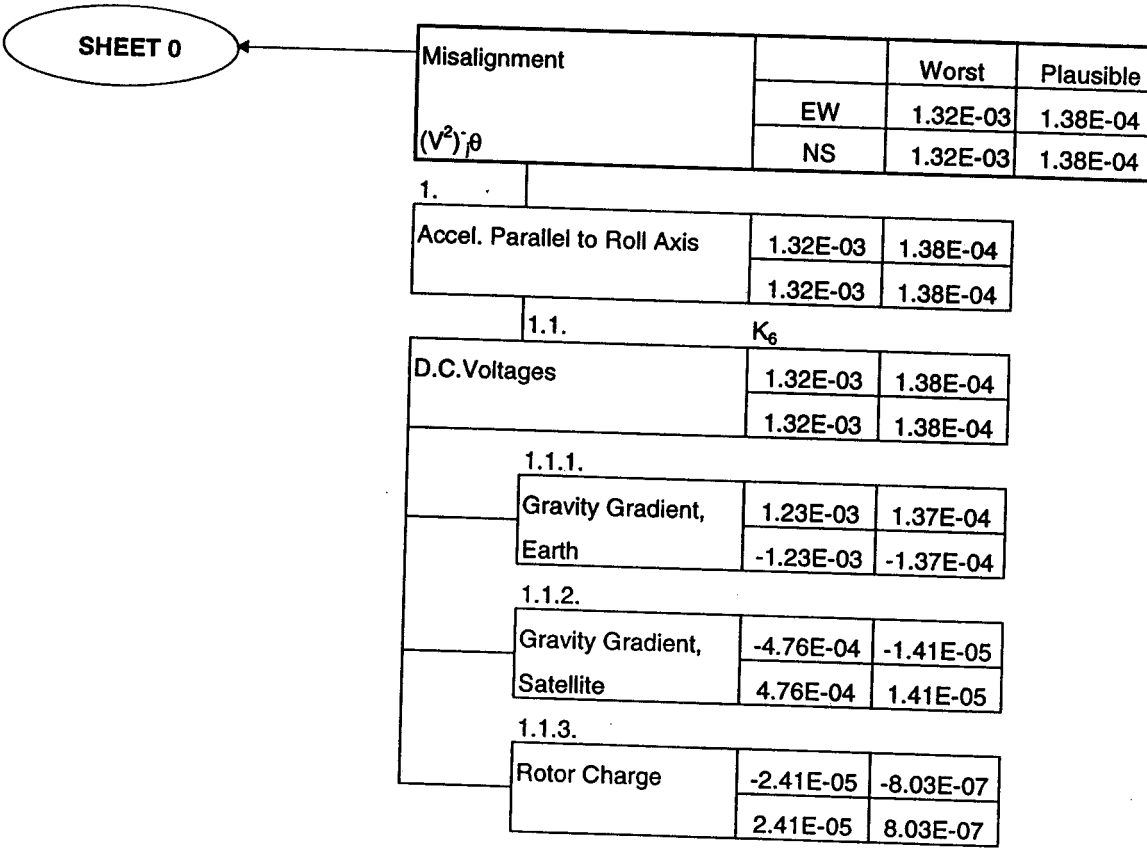

Fig. 3

Support Independent, Housing Fixed, Nominal Position Torques

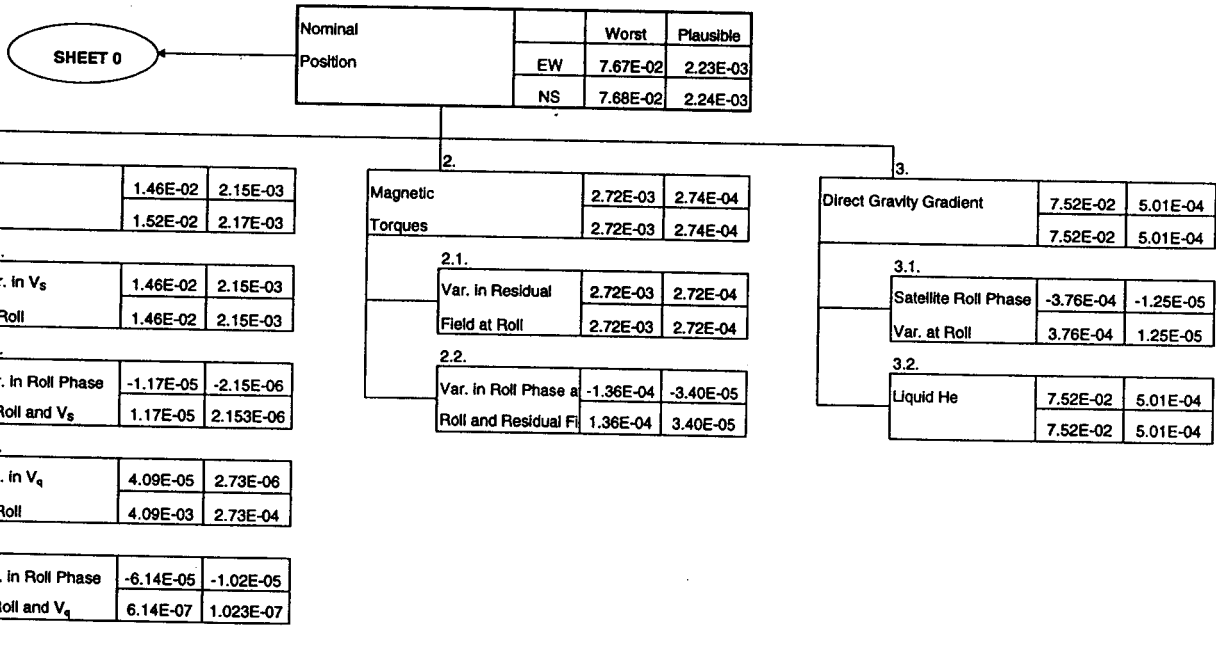

Fig. 4

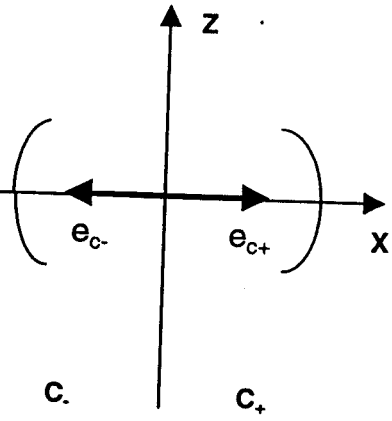

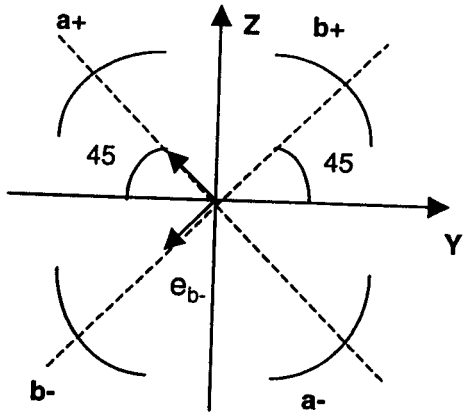

Fig. 5

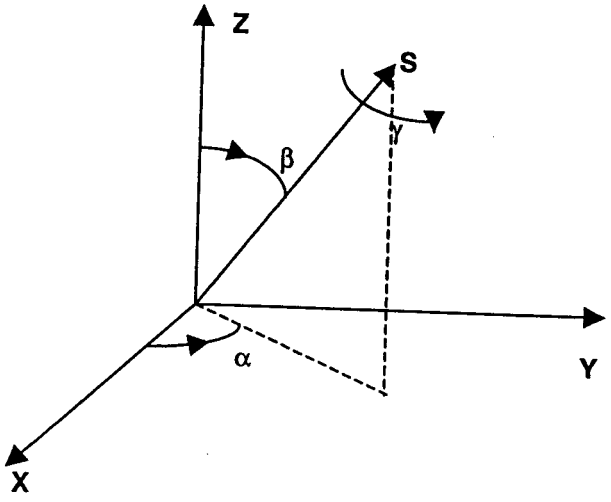

Fig.6

Top Torques (plausible case)				
ory	Sht.	Box	Name / Position	Dr. R. marcs/yr
			I. EW	
	4	1.2.1.	h_a-h_b at roll, Nominal	8.23E-02
	8	2.1.	Coupling with local shield, Misaligned, Housing fixed	6.70E-03
	5	1.1.1.	h_a+h_b , h_c D.C., Misaligned	6.85E-03
	1	1.2.1.	Gravity gradient, Earth, perp. to roll axis, Nominal	1.04E-02
	6	2.1.1.	h_a+h_b , h_c D.C. + Miscentering at roll	7.91E-03
	10	1.1.	Direct gravity gradient, Earth, Inertially fixed	3.56E-03
	7	1.1.	Var. in sensing voltage at roll, Nominal	2.15E-03
	6	2.2.1.	h_a+h_b , h_c at roll + D.C. Miscentering	1.23E-03
			II. NS	
	4	1.2.1.	h_a-h_b at roll, Nominal	8.23E-02
	8	2.1.	Coupling with local shield, Misaligned	6.70E-03
	5	1.1.1.	h_a+h_b , h_c D.C., Misaligned	6.85E-03
	4	1.2.2.3.	Gravity gradient, Earth, g^2_a-g^2_b , Nominal	6.31E-03
	3	2.2.2.	Difference in Miscenter. Amplitudes at ω_r +/- $2\omega_0$	2.99E-03
	7	1.1.	Variation in sensing voltage at roll, Nominal	2.15E-03
	6	2.1.1.	h_a+h_b , h_c D.C. + Miscentering at roll	4.29E-03
	4	2.2.1.	h_a+h_b , h_c at roll, Nominal	1.67E-03
	6	2.1.1.	h_a+h_b , h_c at roll + D.C. Miscentering	1.23E-03

Fig. 7